View metadata, citation and similar papers at core.ac.uk
brought to you by CORE
provided by CERN Document Server

Akn 564: an unusual component in the X-ray spectra of NLSy1 galaxies

T.J.Turner [1,2], I.M. George [1,3], Hagai Netzer [4,5]

ABSTRACT

We present an *ASCA* observation of the narrow-line Seyfert 1 (NLSy1) Arakelian 564. The X-ray light curve shows rapid variability, but no evidence for energy-dependence to these variations, within the 0.6 – 10 keV bandpass. A strong (EW $\sim$ 70 eV) spectral feature is observed close to 1 keV. A similar feature has been observed in TON S180, another member of the NLSy1 class of objects, but has not been observed in broad-line Seyfert galaxies. The feature energy suggests a large contribution from Fe L-shell lines but its intensity is difficult to explain in terms of emission and/or absorption from photoionized gas. The models which predict most emission at 1 keV are characterized by extreme values of column density, Fe abundance and ionization parameter. Models based on gas in thermal equilibrium with kT$\sim$ 1keV provide an alternative parameterization of the soft spectrum. The latter may be interpreted as the hot intercloud medium, undergoing rapid cooling and producing strong Fe L-shell recombination lines. In all cases the physical conditions are rather different from those observed in broad-line Seyferts.

The hard X-ray spectrum shows a broad and asymmetric Fe Kα line of large equivalent width ($\sim$ 550 eV) suggestive of significant emission from the inner accretion disk. The profile can be explained by a neutral disk viewed at $\sim$ 60 degrees to the line-of-sight, contrary to the hypothesis that NLSy1s are viewed pole-on. The large EW of this line, the strong 1 keV emission and the strong optical Fe emission lines all suggest an extreme Fe abundance in this and perhaps other NLSy1s.

1. Introduction

A terminology has developed which names a one extreme of the distribution of Seyfert galaxies narrow-line Seyfert 1 galaxies (NLSy1s), loosely defined as having FWHM Hβ $<$ 2000 km/s; [OIII]/Hβ $<$ 3, and strong FeII emission. These Seyfert galaxies appear to have systematically different, or very extreme X-ray attributes compared to the rest of the Seyfert population (which we dub BLSy1s, for convenience). Examination of X-ray properties across the Seyfert population reveals an anti-correlation between both X-ray index and FWHM Hβ (Boller et al 1996; Brandt et al 1997) as well as between variability amplitude σ^2_{rms} and FWHM Hβ (Turner et al. 1999). In addition to the obvious range of index and variability properties across the Seyfert population, it is interesting to note those X-ray attributes present in only one subset of sources. For example, it is well established that large amounts of absorbing material attenuate

[1]Laboratory for High Energy Astrophysics, Code 660, NASA/Goddard Space Flight Center, Greenbelt, MD 20771

[2]University of Maryland Baltimore County, 1000 Hilltop Circle, Baltimore, MD 21250

[3]Universities Space Research Association

[4]School of Physics and Astronomy and the Wise Observatory, Tel Aviv University, Tel Aviv 69978, Israel

[5]The Institute of Physical and Chemical Research (RIKEN), Hirosawa, Wako, Saitama 351-0198, Japan

the X-ray spectra of many BLSy1s (with varying degrees of ionization), yet there is little evidence of any line-of-sight gas to the nuclei of NLSy1s.

Theoretical attempts to explain the difference in X-ray properties of NLSy1s include the idea that these sources accrete at a higher rate, given their black hole mass, than the rest of the Seyfert population (e.g. Pounds, Done & Osbourne 1995). This may be consistent with the observation of Fe Kα emission from (apparently) highly ionized material in NLSy1s (Comastri et al 1998, Turner et al 1998) and the relatively large rapid X-ray variations. There were also some attempts (Komossa & Greiner 1999) to explain the unusually steep continuum by dusty warm absorbers.

2. ROSAT observations of Akn 564

Arakelian 564 (IRAS 22403+2927, MCG +05–53–012; z=0.024) falls within the NLSy1 "extreme" of Seyfert properties (Osterbrock & Shuder 1982) and has relatively strong Ca II and Fe II emission lines (van Groningen 1993). Akn 564 shows I(Hα)/I(Hβ)=4.4 (similar to many BLSy1s) and [O III]/H$\beta \sim 12$. Walter & Fink (1993) suggested that the unusual UV (λ1375) to 2 keV flux ratio in Ark 564 could be due to absorption of the UV continuum but X-ray data show no evidence for absorption in excess of the Galactic line-of-sight column $N_H(Gal) = 6.4 \times 10^{20}\mathrm{cm}^{-2}$ (Stark et al. 1992). Unusual dust-to-gas ratio and different lines-of-sight to the UV and X-ray continua have also been suggested (Walter & Fink 1993). A *ROSAT* PSPC pointed spectrum shows significant structure indicative of strong emission or absorption effects, although the PSPC data did not allow a distinction to be made between the presence of emission or absorption features (Brandt et al. 1994). Interestingly, Crenshaw et al. (1999) detect absorption lines in SiIV, Lα, NV and CIV, indicating the presence of at least some material in the line-of-sight to the optical emission region. Crenshaw et al (1999) find a one-to-one correspondence between Seyfert galaxies that show intrinsic UV absorption and X-ray "warm absorbers," indicating that these two phenomena are related. Thus the presence of the UV absorber suggests we should search for the signatures of X-ray absorption in Ark 564.

3. ASCA Observation of Akn 564

ASCA (Makishima et al. 1996) has two solid-state imaging spectrometers (SISs) and two gas imaging spectrometers (GISs) at the focus of four co-aligned X-ray telescopes. This instrument combination yields data over a useful bandpass $\sim 0.6 - 10$ keV. Ark 564 was observed over the period 1996 December 23-24. The data were reduced using standard techniques, as described in Nandra et al. (1997a). Data screening yielded effective exposure times ~ 48 ks in the SIS and ~ 51 ks in the GIS instruments. Ark 564 yielded $1.96^{+}_{-}0.01$ ct/s in SIS0 (0.6-10 keV band). In this paper, all energy ranges are given in the observers frame, unless otherwise noted.

The *ASCA* data show significant flux variability (Fig. 1), with factor-of-two changes occurring in the 0.5 – 10 keV flux, over timescales of a few thousand seconds. Construction of a time series with 256s bins yielded a value for "excess variance" $\sigma^2_{rms} = 39.3^{+}_{-}2.24 \times 10^{-3}$ (see Turner et al. 1999, and references therein for a definition of this quantity and discussion of results for a sample of NLSy1s). Rapid variations of this amplitude are a property of NLSy1s (e.g. Boller et al. 1996). Light curves were also constructed in two different energy bands, 2-10 keV and 0.5-2 keV, and the excess variance compared in the two bands. This test was prompted by the discovery of energy-dependent variability in Ton S180, where the strongest X-ray variations appear to be

observed in the soft X-ray band. However, we found no evidence for energy-dependent variability in Ark 564.

The X-ray spectrum is remarkable. The continuum slope was determined by fitting an absorbed power-law to the 0.6-5.0 plus 7.5-10.0 keV band (to avoid confusion due to the Fe Kα line). Fig 2 shows residuals compared to that power-law fit. A strong spectral feature is evident at ~ 1 keV and an excess of emission close to 7 keV, which we know to be due to an unmodeled Fe Kα line. The photon index over the (featureless) 1.5-4.5 keV band is $\Gamma = 2.63^{+0.16}_{-0.03}$ (and probably provides the best measure of the underlying continuum slope).

3.1. The soft X-ray spectrum

The observation of a strong spectral feature close to 1 keV is especially interesting. A similar feature has been observed in the bright NLSy1 TON S180 (Turner, George & Nandra 1998). Features of this nature have not been observed in BLSy1s, but something consistent with the same feature has been seen at low S/N in some QSOs (Fiore et al 1998; George et al. 1999). The data (excluding the 5.0 – 7.5 keV band) were successfully modeled using a power-law continuum plus Gaussian emission feature. The best fit gave $\Gamma = 2.62^{+0.01}_{-0.02}$ with continuum normalization $n = 1.96^{+0.02}_{-0.04} \times 10^{-2}$photons cm^{-2}s^{-1} at 1 keV; no (neutral) absorption was found in excess of the Galactic value, and the rest-energy of the Gaussian was $E = 0.99^{+0.02}_{-0.04}$ keV with width $\sigma = 0.16^{+0.03}_{-0.02}$ keV and normalization $n = 1.3^{+0.3}_{-0.1} \times 10^{-3}$photons cm^{-2}s^{-1}. The equivalent width (EW) of this feature is $\sim 70^{+20}_{-10}$ eV compared to the observed continuum level. This fit gave $\chi^2 = 1332/1261$ degrees of freedom (dof). To ensure that the strength of the low energy feature is not related to any instrumental effects in the detectors, we thoroughly investigated sub-divisions of the data based upon instrumental parameters, these efforts are described in the Appendix.

Intensity-selected spectra revealed no significant variability in this spectral feature during the observation. However, we note that the source was in a high flux state for a relatively short time, affording no strong constraints on spectral variations.

We attempted some alternative fits where the spectrum of Ark 564 is parameterized by a double power-law with imprinted absorption edges. (We do not discuss models using absorption edges in conjunction with a single power-law, as these were totally inadequate). It is interesting to compare these fits with similar ones performed on the PSPC data (Brandt et al. 1994) especially in light of an expectation that we might observe absorption in the X-ray band associated with the absorption systems detected in the UV data (Crenshaw et al. 1999). We find the *ASCA* spectra are not adequately fit by a model composed of a double power-law with neutral absorber, plus single absorption edge. Such a model yielded $\chi^2 = 1546/1260$ dof (again excluding the 5.0 – 7.5 keV band) and an edge energy $E = 0.60$ keV (i.e. it hit the lower bound allowed for the edge energy) with optical depth $\tau = 0.73$. The fit statistic is $\Delta\chi^2$ of 214 worse than that obtained when fitting the feature with a Gaussian emission profile (above), and the latter does not require the presence of a second power-law continuum component. Addition of a second edge to the model yields an improvement to the fit, giving $\chi^2 = 1395/1258$ dof, with the second edge energy $E = 1.32$ keV and optical depth $\tau = 0.15$. This fit is $\Delta\chi^2$ of 63 worse than the fit utilizing an emission feature and so we do not pursue this line of modeling. This conclusion is in agreement with that stated in recent work by Vaughan et al (1999), who find signatures of warm absorbers in several NLSy1s, but find the features in Ark 564 to be better modeled with emission than absorption features.

The energy of the Gaussian emission component suggests the observed feature is a blend

of line emission from the K-shells of O and Ne, and the L-shell of Fe, thus we investigate the agreement between the data and realistic physical models which produce strong emission from those elements.

3.1.1. Photoionized Gas

We attempted to model the emission assuming an origin in photoionized gas in equilibrium using models calculated by ION97, the 1997 version of the code ION (see Netzer 1996). Emission features could dominate over absorption features if the ionized gas is out of the line-of-sight. We allowed the material to be photoionized by the $\Gamma \sim 2.6$ continuum of Akn 564. This steep ionizing continuum yields an emission spectrum characteristically different from "typical" warm absorber models, like the ones illustrated in several of our previous publications (Netzer 1996; George et al 1998). In this case it is characterized by much larger column density and larger U_X than found for Seyfert 1 galaxies (cf George et al. 1998). We will not expand on this point which is currently under study.

The modeling of the blend of lines around 0.8–1.2 keV is complicated by the rich spectrum of the Fe XVII – XXI L-shell lines; there are dozens energy levels and hundreds of transitions to be considered. Great effort has been made by Liedahl and collaborators (e.g. Kallman et al. 1996 and references therein) to calculate the atomic data required for such modeling. Previous versions of ION included only 2-5 Fe recombination lines per ion (Netzer 1996). We have extended the list by grouping a detailed line list, generously provided by D. Liedahl, into 8-12 lines per ion such that the total recombination emission is identical to the one computed by the more sophisticated atomic models; this allows a reasonable simulation of the Fe recombination spectrum (adequate, given the *ASCA* spectral resolution). These models do not yet contain the contribution due to continuum fluorescence (absorption of continuum radiation by resonance lines) which, in some geometries, can approximately double the line intensities. The details of this contribution are currently under investigation.

We used trial models composed of a continuum power-law plus emission from ionized gas. Emission models were generated covering a column density range of $10^{22} - 10^{23.75}$ cm^{-2}; ionization parameter U_x in the range 0.1–10.0 (see George et al. 1998 for a definition of U_x) and covering fraction $C_f = 0.1$–1.0. The models that produce the largest summed 0.75–1.2 keV flux are those with $C_f \simeq 0.5$, column density of about $10^{23.5}$ cm^{-2} and U_x of 5 – 10. These models typically give (for solar composition) a line blend (summing lines and recombination continua in the 0.75–1.2 keV range) with EW $\simeq$ 20 eV. This EW is measured relative to the unobscured continuum and a larger EW, by up to a factor 1.2, is measured relative to the observed continuum (which is somewhat suppressed due to absorption). These models did not provide an adequate fit to the data. The best fit which was achieved (for solar abundances) was that utilizing the pure emission spectrum from the photoionized gas which yielded $\chi^2 = 1701/1260$ *dof* (excluding the Fe K-shell band) for emission from a column of gas with $N_H = 3.0^{+1.6}_{-0.6} \times 10^{23}$ cm^{-2} and $U_x = 10^{+}_{-}1$. Fig. 3 shows the data and model illustrating how little of the observed feature can be explained. In these models production of a strong feature at 1 keV leads to the expectation of strong features at other energies – ruled out by the *ASCA* spectral data. We have also explored the possibility that the Fe abundance in this source is unusually high. This is motivated by the strong Fe Kα line and the strong optical FeII lines in NLSy1s. Doubling the Fe abundance results in $\sim 50\%$ increase in the EW, bringing it close to $\sim$ 30 eV, but still falling short of the strength of the observed feature.

None of the models based upon the emission spectrum from photoionized gas provided an adequate fit to the data. Although models utilizing simple absorption edges failed to fit the data, we considered the effects of absorption by a cloud of photoionized gas. A photoionized cloud produces an absorption profile which is obviously different to that of arbitrary absorption edges considered in isolation. We considered both models where a single and a double power-law continuum were absorbed by a cloud of photoionized gas. Fits were performed with and without an unconstrained contribution from the emission spectrum of that gas. However, none of these models produced a satisfactory fit to the data.

3.1.2. Thermal Gas

Next we considered emission from gas in thermal equilibrium. ION does not include a very sophisticated treatment of collisionally excited transitions in Fe XVII – XXIII; instead it groups those lines into bands containing very small number of lines per ion. The overall collisional contribution is maintained assuring energy conservation. This is not adequate for obtaining the realistic emissivity pattern of the Fe L-shell transitions. We have therefore used the MEKAL calculations, in XSPEC, to model the 0.8–1.2 keV thermal emission, as an alternative to the model from ION. We note that such calculations, while very detailed, do not include optical depth effects that are important for some lines. Such models provide a reasonable fit to the bulk of the soft feature. A model composed of a continuum power-law plus MEKAL component gave a best-fit temperature $kT = 1.07^{+}_{-}0.04$ keV for the gas (assuming cosmic abundances) with $\chi^2 = 1453/1262$ dof. While this is statistically superior to the fit using a power-law plus ION, we note that neither model matches the entire flux in the soft hump. As expected, for this temperature the dominant Fe ions are Fe XVI – XX and the resulting Fe line complex around 1 keV is very strong. In this model, the flux in the thermal component (0.5 – 2 keV band) is $f_{0.5-2} = 2.5 \times 10^{-12}$erg cm^{-2} s^{-1} with a corresponding luminosity $L_{0.5-2} = 7 \times 10^{42}$erg s^{-1} (assuming $H_0 = 50$km s^{-1} Mpc^{-1}, q$_0 = 0.5$). While the *ROSAT* PSPC data were taken at a different epoch, we compared those data with this model, to see whether there was any inconsistency if the model was extrapolated down to 0.1 keV, specifically, to determine whether the PSPC data fell below the flux of the MEKAL component, which would provide significant constraints to our model. The PSPC data gave good agreement with the *ASCA* model in the 0.1 -0.5 keV band. We review the possible origins of this component in the discussion.

3.2. Fe Kα

A significant Fe Kα emission line is evident in the *ASCA* spectrum (Fig. 2). The line profile is asymmetric with a marked red wing, as observed commonly in Seyfert 1 galaxies (Nandra et al. 1997b). The line was modeled using a broad Gaussian component. This provided an adequate parameterization of the line shape, and yielded a rest-energy for the line $E = 6.25^{+}_{-}0.29$ keV, line width $\sigma = 1.0^{+0p}_{-0.12}$ keV, normalization $n = 9.28^{+}_{-}2.11 \times 10^{-5}$photons cm^{-2} s^{-1} and equivalent width $EW = 566^{+}_{-}128$ eV (the p denotes that the parameter hit the hard bound set within the fit).

The asymmetry of the line lead us to fit a disk-line model profile (Fabian et al. 1989). The model assumes a Schwarzschild geometry and we assumed an emissivity law r^{-q} for the illumination pattern of the accretion disk, where r is the radial distance from the black hole, and q=2.5 (as found for a sample of Seyfert 1 galaxies; Nandra et al. 1997b). We assume the

line originates between 6 and 1000 gravitational radii and we constrained the rest-energy of the line to lie between 6.4 and 7 keV. The inclination of the system is defined such that $i = 0$ is a disk orientated face-on to the observer. This model gave a marginally worse fit than the broad Gaussian model for the same number of free parameters ($\Delta\chi^2 = 4$ for 1217 degrees of freedom). The rest-energy of the line was $E = 6.40^{+0.15}_{-0p}$ keV, the inclination was $i = 57^{+21}_{-8}$ degrees and normalization $n = 7.09^{+2.02}_{-1.79} \times 10^{-5}$photons cm^{-2} s^{-1}. The equivalent width was $EW = 550^{+128}_{-156}$ eV. In both parameterizations of the line, we obtain a flux of $\sim 9 \times 10^{-13}$erg cm^{-2} s^{-1}, corresponding to a line luminosity $L \sim 2.5 \times 10^{42}$erg s^{-1}.

4. Discussion

The strong spectral signature in the soft X-ray regime is intriguing. Starburst activity could explain the presence of a large soft X-ray flux, and such activity often appears concentrated towards a galaxy center. The large X-ray luminosity of this component would suggest that it must produce detectable infrared emission if these X-rays originate from a starburst region. In the 0.5 – 4.5 keV band the luminosity in the soft component alone is 8×10^{42}erg s^{-1}. Use of this bandpass allows comparison with a study of normal and starburst galaxies (David, Jones & Forman 1992). Using the infrared fluxes reported for Ark 564 (Bonatto & Pastoriza 1997) the estimated X-ray emission from a region dominated by star formation would be $L_{0.5-4.5} \sim 6 \times 10^{40}$erg s^{-1}, almost two orders of magnitude lower than that observed. Using again the infrared fluxes from Bonatto & Pastoriza (1997) we calculate indices $\alpha_{60,25} = -0.642$ and $\alpha_{100,60} = -0.204$ [6]. We compared these indices with those calculated for samples of Seyfert galaxies and starburst dominated galaxies (Miley, Neugebauer & Soifer 1985). The 60μm curvature is not consistent with that observed in starburst galaxies (c.f. Miley, Neugebauer & Soifer 1985; their Fig. 4). Thus the infrared luminosity and spectrum indicate that starburst activity does not make a significant contribution to the observed X-ray luminosity in Ark 564.

The optical image of Ark 564 does show extent with ridges of enhanced emission with a red optical color (Arakelian, 1975). The extended optical features give Ark 564 a diameter of $\sim 30''$, with $12''$ separating the nucleus from one bright optical region to the SE. The *ROSAT* HRI image of this source shows no significant extended emission coincident with the optical enhancements. The *ROSAT* HRI data provide an upper limit such that the emitting gas must exist within the inner ~ 3 kpc of the nucleus, much stronger constraints will be obtained by AXAF images in the near future. (Unfortunately faint extent would be very difficult to confirm with the HRI, because the instrument suffers some scattering of point-source photons into a halo outside of the point-spread-function.) An extended thermal source would not show rapid time variability. While we see strong X-ray flux variability in Akn 564 it is currently unclear whether the flux in the spectral feature itself varies. The current constraint, that the hot gas lies within a 3 kpc radius, leaves many possibilities open to discussion. However, no such component is observed in normal galaxies or BLSy1s, thus it seems more compelling to discuss possible origins associated with the nucleus, rather than further out (such as gas in the galactic halo).

The *ASCA* data show the spectral feature at 1 keV is not produced by emission or absorption from gas in photoionization equilibrium. An alternative is that the gas is in thermal equilibrium. The MEKAL model can be extrapolated to give a bolometric luminosity in that

[6] $\alpha_{x,y} = -log[\frac{F_\nu(y)}{F_\nu(x)}]/log[\frac{\nu(y)}{\nu(x)}]$

component (over $\sim$ 0.1-10 keV, although contributing little above 2 keV) which is 10^{43}erg s^{-1} (c.f. the nuclear luminosity $L_{2-10} \sim 5 \times 10^{43}$erg s^{-1}). The temperature determined from our modeling is $kT = 1$ keV. This can be explained if the gas exists in a location where some heating mechanism dominates over photoionization heating. This could be part of the nucleus obscured from the central radiation field or a location where the density is high enough that collisional cooling is able to maintain a low level of ionization. This would give rise to strong line emission.

We consider an alternative origin as the hot intercloud medium (HIM) confining the clouds in either the broad line region (BLR) or narrow line region (NLR). Such gas has been postulated in early studies of AGN. Krolik, McKee and Tarter (1981) discuss the expectation that emission line clouds must be confined by a hot (10^7 – 10^9K) medium (also see Netzer 1990 and references therein). This medium has also been discussed in connection with warm absorber gas in AGN, by Reynolds and Fabian (1995). The situation regarding NLSy1 is of particular interest since the HIM is likely to be at relatively low temperature due to the inefficient Compton heating (because of the very soft X-ray continuum) and the large Compton cooling (due to the strong UV bump). Such material, if in equilibrium, does not emit strong emission lines since it is fully ionized. However, the HIM may be unstable. NLSy1s are known to have large flux variations and it is conceivable that the current observed state of Akn 564 represents a low-phase of activity. Previous higher luminosity phases might have resulted in full ionization of the HIM which, at the time of the *ASCA* observations was undergoing intense cooling and recombination. The recombination time depends on the density and temperature. Given a BLR location, and a temperature of 10^6K, the recombination time is short enough to produce a strong recombination spectrum. Full modeling of such a time-dependent component is beyond the scope of this paper. We note, however, that non-equilibrium situations are likely to be important in some cases involving rapidly varying sources (Nicastro et al. 1999).

The assumption that there is a strong thermal component in Akn 564 can be put to observational tests. First, this component is unlikely to respond on short time scales to large continuum variations. Its relative contribution at high phases of the source should decrease inversely with the continuum brightness. Second, high resolution spectral observations, like those expected with several of the coming X-ray missions (*Chandra* and *XMM*), will provide clear diagnostic tools to allow the identification of the thermal plasma and its separation from any photoionized plasma. If thermal gas is indeed found in high resolution observations of Akn 564, it will provide yet another clue to the unique spectral appearance of NLSy1 galaxies.

Turning now to the properties of the Fe Kα line in Ark 564, we note an asymmetric shape as observed in BLSy1s. The pronounced red wing indicates that the innermost disk is emissive. We find an acceptable explanation of the Fe Kα line as emission from an accretion disk composed of neutral material, but viewed at $\sim$ 60 degrees to the line-of-sight. This inclination angle contradicts the popular hypothesis that NLSy1s are Seyfert nuclei viewed pole-on. Data from Ark 564 and Ton S180 indicate that the Fe Kα lines may have systematically large equivalent width in NLSy1s, compared to BLSy1s. The unusual spectral feature observed at 1 keV in these two NLSy1s is consistent with emission lines from the L-shell of Fe. Ark 564 and Ton S180 show strong optical FeII emission, as do NLSy1 galaxies in general. These facts suggest that overabundance of Fe may be a property of NLSy1s.

5. Conclusions

An *ASCA* observation of the NLSy1 galaxy Ark 564 reveals rapid X-ray variability, although we find no evidence for energy-dependent flux changes. Ark 564 has a complex X-ray spectrum. A strong feature is observed close to 1 keV, which is not easily attributed to emission or absorption by photoionized gas or emission from gas in thermal equilibrium. A similar feature was previously observed in Ton S180, these features may be characteristic of NLSy1s and important to understanding conditions in these sources. The emission may indicate the hot intercloud medium in the BLR or NLR is currently in a cooling phase in Ark 564. The hot intercloud medium may have a characteristically different temperature in NLSy1s to the rest of the Seyfert population, affording a visible signature of the gas in the soft X-ray spectrum of NLSy1s, but not BLSy1s. Separation of Ne and Fe lines over the 0.8–1.2 keV range with *XMM* or *Chandra* grating observations will enable us to test this explicitly.

Ark 564 has a broad and asymmetric Fe Kα line of large equivalent width, $\sim$ 550 eV. The line profile is consistent with emission from a neutral disk inclined at 60 degrees to our line-of-sight which argues against models inferring NLSy1s are viewed pole-on.

Appendix

We investigated whether the strength and shape of the low energy feature in Ark 564 changed as a function of any instrumental parameter. First we examined each of the SIS detectors. As the lower level for event discrimination changed during the observation we accumulated two spectra for each SIS, one for each discriminator level. A separate response matrix was generated for each SIS and for each discriminator level. These four SIS spectra were then fit to the power-law model, and the data/model ratios are shown in Fig. 4. The SIS0 and SIS1 data are shown separately. It is clear that the spectral feature is evident in both, showing consistent strength in each. Fig. 4 shows a comparison between spectra from each discriminator level, for the two SIS instruments, demonstrating the close consistency between each pair. As no significant difference was found, henceforth we show only the average SIS0 spectrum and average SIS1 spectrum. The known discrepancy between SIS0 and SIS1 data is evident. SIS1 data lie 10% lower than SIS0 data below an energy of $\sim$ 0.8 keV. However, the peak and turnover energy of the low energy feature are clearly seen in SIS0, therefore the overall shape and strength of the feature is not an artifact of problems with SIS1. We found no difference in our conclusions considering SIS0 data alone, and as there are small uncertainties in all instruments, we consider the best approach to be that which we present, analysis based upon simultaneous fits to the four *ASCA* instruments.

There are also documented problems with the SIS response matrix generator for 2-pixel events in cases when the event threshold is high. There has been some speculation that a more reliable analysis can be achieved by consideration of the grade 0 events alone (for which accurate response matrices can be generated regardless of event threshold), therefore we repeated our analysis using only the grade 0 events. Fig. 4 shows the data/model ratio for SIS0 and SIS1 separately, for spectra accumulated from grade 0 events alone. We find no dependence of the strength of the feature on grade of event.

The data were also subdivided based upon the CCD temperature during the observation. We found no changes in the strength of the low energy feature as the CCD temperatures changed. To illustrate this point we show data/model ratios to the power-law model, for two SIS1 spectra; the first accumulated for a mean instrument temperature of -60C, the second for mean

temperature -61 C (close to the full range of temperature during the observation).

In conclusion, we have screened and subdivided the data based upon a large number of different criteria, but found no instrumental effects which falsely enhanced the strength of the low energy feature. Our conclusions are not dependent on the small residual uncertainties in the *ASCA* calibration.

6. Acknowledgements

We are grateful to the *ASCA* team for their operation of the satellite. This research has made use of the NASA/IPAC Extragalactic database, which is operated by the Jet Propulsion Laboratory, Caltech, under contract with NASA; of the Simbad database, operated at CDS, Strasbourg, France; and data obtained through the HEASARC on-line service, provided by NASA/GSFC. This work was supported by NASA Long Term Space Astrophysics grant NAG 5-7385.

References

Arakelian, M.A. 1975, SoByu 47, 3
Boller et al 1996A&A, 305, 53
Bonatto, C.J., Pastoriza, M.G. 1997, ApJ 486, 132
Brandt, W.N., Fabian, A.C., Nandra, K., Reynolds, C.S., Brinkmann, W. 1994, MNRAS, 271, 958
Brandt et al 1997 MNRAS, 285, 25
Comastri et al 1998, A&A, 333, 31
Crenshaw, D.M., Kraemer, S.B., Boggess, A., Maran, S.P., Mushotzky, R.F., Wu, C-C. 1999, ApJ 516, 750
David, L.P., Jones, C., Forman, W. 1992, ApJ 388, 82
Fabian,A.C., Rees, M.J., Stella, L., White, N.E. 1989, MNRAS 238, 729
Fiore,F., et al. 1998, MNRAS 503, 607
George, I.M., Turner,T.J., Netzer, H., Nandra, K., Mushotzky, R.F., Yaqoob, T. 1998, ApJS 114, 73
George, I.M., et al 1999, ApJ, in prep
Kallman, T. R., Liedahl, D., Osterheld, A., Goldstein, W., Kahn, S. 1996, ApJ 465, 994
Komossa, S., Greiner, J. 1999, (Astro-ph9810105)
Krolik, J.H., McKee,C.F., Tarter,C.B. 1981, ApJ 249, 422
Makashima, et al. 1996, PASJ 48, 171
Miley,G.K., Neugebauer, G., Soifer, B.T. 1985, ApJ 293, 148
Nandra, K., George,I.M., Mushotzky, R.F.,Turner,T.J.,Yaqoob, T. 1997a, ApJ 476, 70
Nandra, K., George,I.M., Mushotzky,R.F., Turner,T.J., Yaqoob,T. 1997b, ApJ 477, 602
Netzer,H. 1990, in *Active Galactic Nuclei*, by Woltjer, Netzer & Blandford, SAA-FEE series, Courvoisier and Mayor eds (Berlin, Springer) p57
Netzer, H. 1996, ApJ 473, 781
Netzer, H. 1999, in prep
Nicastro, F., Fiore, F., Perola, G.C., Elvis, M., 1999, ApJ 512, 184
Osterbrock, D.E., Shuder, J.M., 1982, ApJS 49, 149
Pounds, K.A., Done, C., Osbourne, J.P., 1995, MNRAS 277, L5

Reynolds, C., Fabian, A.C. 1995, *M. N. R. A. S.* 273, 1167
Stark, A.A., Gammie, C.F., Wilson, R.W., Bally, J., Linke, R.A., Heiles, C., Hurwitz, M., 1992, ApJS 79, 77
Turner, T.J., George, I.M., Nandra, K. 1998, ApJ, 508, 648
Turner, T.J., George, I.M., Nandra, K. 1999, ApJ, sched. Nov 1 issue, astro-ph/9906050
Van Groningen, E. 1993, A&A 272, 25
Vaughan, S., Reeves, J., Warwick, R., Edelson, R. 1999, MNRAS in press
Walter, R., Fink, H.H., 1993, A&A 274, 105

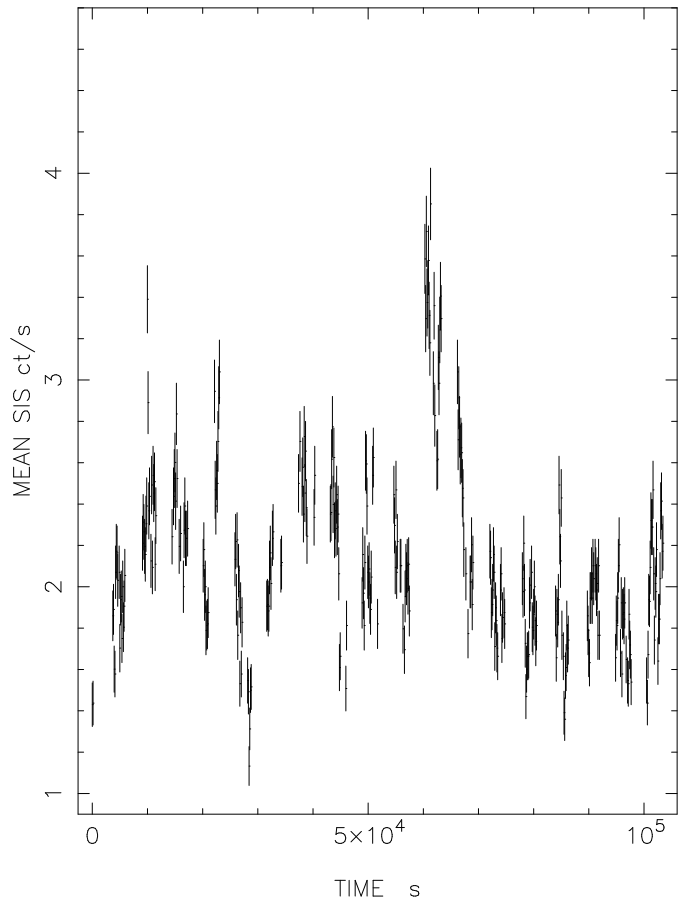

Fig. 1.— *The ASCA light curve in the 0.5-10 keV band, based upon the combined SIS data, in 128 s bins.*

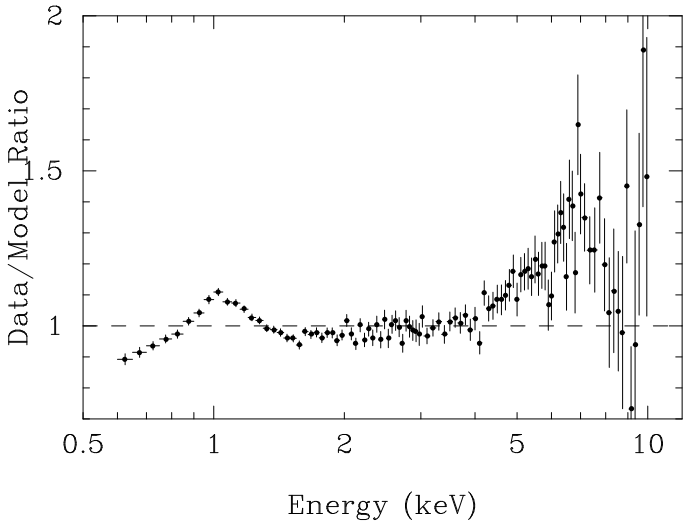

Fig. 2.— *The data/model ratio (combined SIS and GIS data) compared to a power-law continuum fit to the 0.6-5.0 plus 7.5-10.0 keV ASCA data, with the 5.0 – 7.5 keV data overlaid for comparison. Residual counts due to emission from Fe Kα are evident, as well as the strong feature close to 1 keV.*

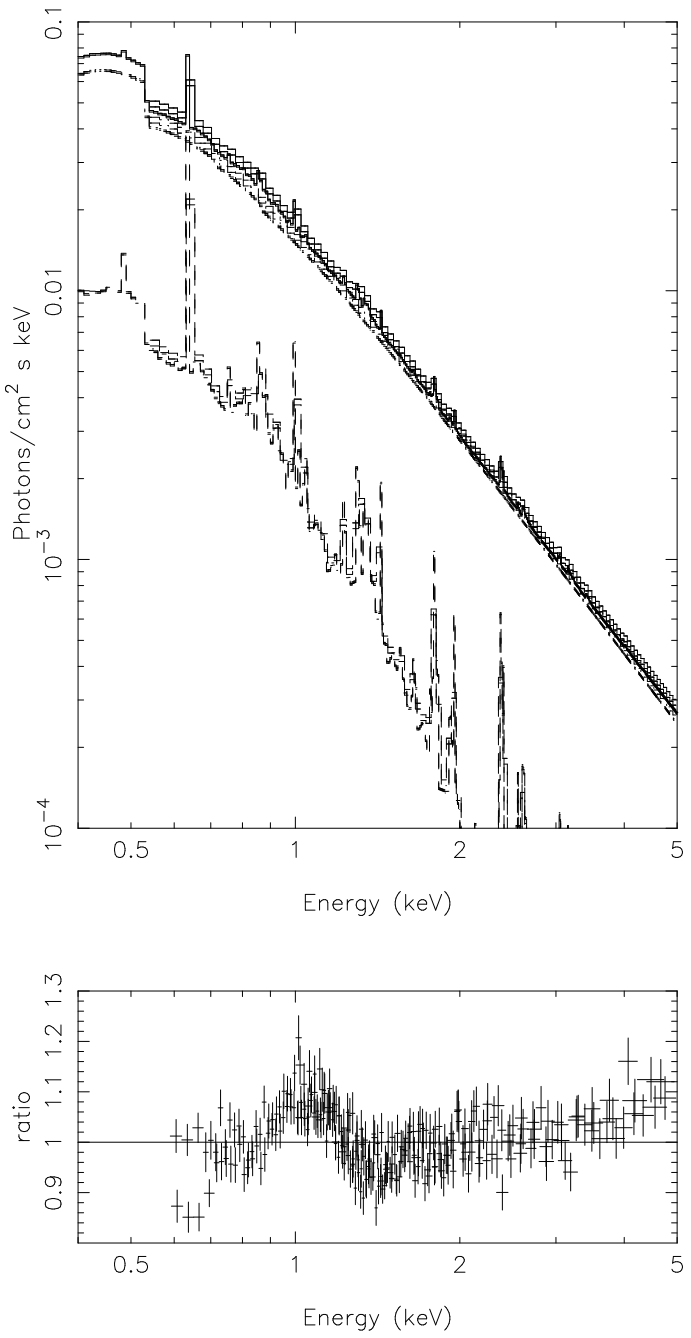

Fig. 3.— *Top: The model for the best fit using the photoionized gas, as detailed in §3.1.1. Bottom: The data/model ratio with each of the four instruments plotted*

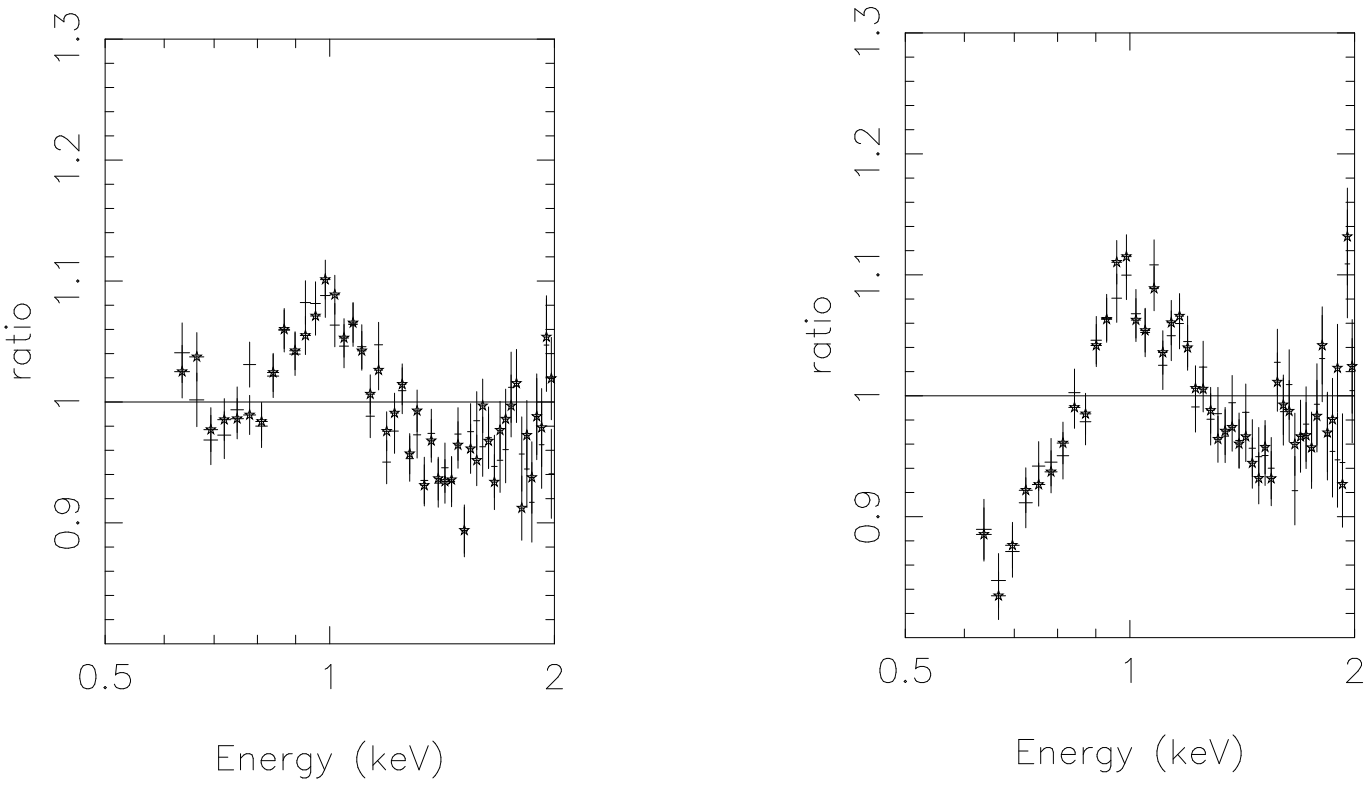

Fig. 4.— *The data/model ratio as in Figure 2, except that data are shown for each individual SIS and each level discriminator used during the observation. Left: SIS 0, stars are data where S0LVDL=135, the crosses are S0LVDL=115. Right: SIS 1, the stars show S1LVDL=146, the crosses are S1LVDL=125*

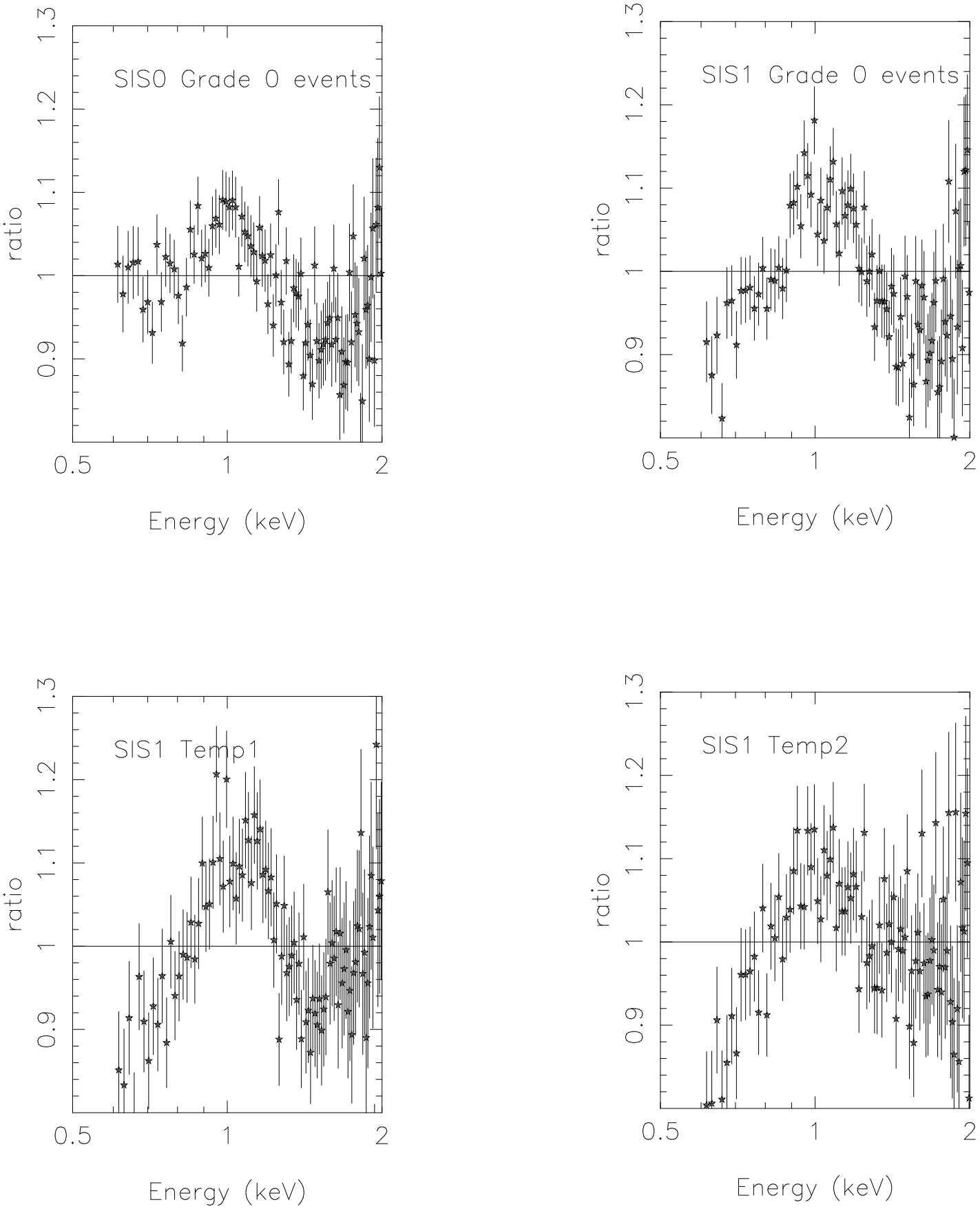

Fig. 5.— *Data/model ratio as in Figure 2. Top: Grade 0 data from SIS 0 and SIS 1. Bottom: Data/model ratio for SIS 1 subdivided by CCD temperature, T1=-60 C (left) and T2=-61 C* (right)